Available online at www.sciencedirect.com
SCIENCE DIRECT®

Journal of the European Ceramic Society 23 (2003) 2105–2111
www.elsevier.com/locate/jeurceramsoc

Influence of particle size on the conductance of SnO_2 thick films

M.A. Ponce, C.M. Aldao, M.S. Castro*

Institute of Materials Science and Technology (INTEMA), (CONICET—Universidad Nacional de Mar del Plata), Av. Juan B. Justo 4302 (B7608FDQ), Mar del Plata, Argentina

Received 5 June 2002; received in revised form 20 December 2002; accepted 13 January 2003

Abstract

The electrical response of SnO_2 thick films was found to be highly dependent on the grain size. This result can be explained as the consequence of the type of intergranular potential barriers developed at intergrains. Specifically, samples with smaller particle size have overlapped potential barriers and samples with higher particle size have separated potential barriers. Also, the influence of gas transport phenomena on the resistance of the gas sensor was investigated. From an analysis of the possible mechanisms involved in the oxygen diffusion, the Knudsen diffusion is suggested as the controlling step.

Keywords: Defects; Diffusion; Electrical properties; Films; Grain size; Sensors; SnO_2

1. Introduction

Gas sensors based on semiconducting metal oxides are devices which present a change in the resistivity with the gas exposure. The sensing mechanism involves an electrical conductance change caused by gas adsorption on the semiconductor surface, which is highly dependent on the surface stoichiometry.[1] Also, the sensing properties are influenced by the microstructural features, such as the grain size of semiconductor particles, the geometry, and the connectivity between particles.[2] Sensors based on tin oxide are widely used for detection of oxidising or reducing gases. On this matter, disks, thick and thin films have been used to construct this type of sensors.[3] Beside the technological progresses in tin oxide gas sensors, basic understandings of semiconductor interfaces have also deepened through the elucidation of the role of Schottky barriers and adsorbed oxygen, grain size effects, and chemical and electronic sensitisation mechanisms.[4] Thus, Maekawa et al. have determined that the sensitivity and selectivity to gases depend strongly on the grain size, and the selectivity is improved by growing the grain size.[5]

Gas sensors are provided as a porous sensing layer of a semiconductor oxide. Oxygen diffuses in the sensing layer where is adsorbed on the grain surface. Then, the gas concentration inside the sensing layer would decrease with the diffusion depth. As a consequence, the transient response of the sensor is directly affected by the gas diffusion rate.[6]

It is known that the n-type semiconducting behaviour of tin oxide is due to oxygen vacancies that act as donors. In these materials, electrical conduction is determined by grain boundary barriers that depend on the amount of chemisorbed oxygen. Oxygen chemisorbed from the atmosphere forms charged species and then electrons are trapped at the grain boundaries modifying the potential barriers. Reducing gases remove some of the adsorbed oxygen, the potential barriers are changed and then the overall conductivity, originating a sensor signal.[7–10]

In this paper we present a study of the influence of the grain size on the conduction process in SnO_2 thick films. Electrical conductance as a function of temperature during heating and cooling of the film and transients at step isothermal changes in oxygen pressure are presented. Also, an interpretation of the possible diffusion processes is discussed.

2. Experimental

Commercial high-purity SnO_2 (Aldrich, medium particle size 0.4 μm) was ground until a medium particle

* Corresponding author.
E-mail addresses: mcastro@fi.mdp.edu.ar (M.S. Castro), mponce@fi.mdp.edu.ar (M.A. Ponce), cmaldao@fi.mdp.edu.ar (C.M. Aldao).

0955-2219/03/$ - see front matter © 2003 Elsevier Science Ltd. All rights reserved.
doi:10.1016/S0955-2219(03)00037-2

size of 0.1 μm (labelled powders P1). A calcination process carried out at 1100 °C for 2 h led to powders with larger particle size (labelled powders P2). Then, a paste was prepared with an organic binder (glycerol) and the powders P1 and P2. The used solid/organic binder ratio was $\frac{1}{2}$. No dopants were added. Thick, porous film samples were made by painting onto insulating alumina substrate on which electrodes with an interdigit shape has been deposited by sputtering. Finally, samples were thermally treated for 2 h in air at 500 °C. Samples were labelled S1 (small particle size) and S2 (high particle size). The thick of the films was measured using a coordinates measuring machine Mitutoyo BH506.

To image the tin oxide surfaces a Philips 505 SEM and a commercial scanning tunnelling microscopy (STM) Nanoscope II were employed. The STM can be operated at air pressure under different gases or mixtures. A platinum–iridium tip was used for imaging. All experiments were conducted in the dark with the microscope placed on a vibratory-isolated optical table. Samples were secured with a small metallic clip connected to the microscope ground. A sample-tip voltage of 8V and a current of 0.5 nA were used to acquire the STM images. Samples images were successfully acquired under a nitrogen atmosphere. Size particle distributions of the powders were determined by the Sedigraph technique with a Micromeritics.

Resistance vs. time curves were measured while changing the vacuum into air flux and, after having reached quasi-saturation, changing the oxygen flux back into vacuum. In temperature cycling experiments, resistance was measured while raising and then decreasing the temperature from room temperature up to 400 °C at a rate of ~2 °C/min with the sample kept in oxygen (8.4 mmHg).

3. Results and discussion

Table 1 shows data from particle size distributions corresponding to powders P1 and P2. We considered that D90, D50 and D10 are the corresponding diameters of 90, 50 and 10% volume respectively, and $W = (D90 - D10)/D50$ is a measure of the distribution width of particle size. From Table 1 it is apparent that the increasing in the particle sizes is significant after the powder calcination at 1100 °C. Also, powders P2 have a wider particle size distribution.

Table 1
Particle size distributions of the powders P1 and P2

Sample	D20 (μm)	D50 (μm)	D80 (μm)	W
P1	0.15	0.42	0.88	1.74
P2	0.26	0.68	3.3	4.47

In Fig. 1 SEM micrographies of the samples S1 and S2 are shown. Both samples present homogeneous microstructures. From SEM micrographs a significant difference in the microstructures of S1 and S2 is observed. Both samples showed the presence of agglomerates, but samples made with higher particle size (S2) showed a highly porous microstructure with the presence of some cracks (not showed in this figure). From Fig. 1A, the average particle size of sample labelled S1 was determined to be between 100 and 250 nm, while for sample labelled S2 it was determined to be between 250 and 420 nm. However, using STM we observed that we are dealing with particle agglomerates having a mean particle size of 50 nm in sample S1 (see Fig. 2). The mean thick of the films was 100 μm for sample S1 and 440 μm for sample S2.

Fig. 3 shows the electrical response (resistance vs. time) of the sample with smaller particle size after

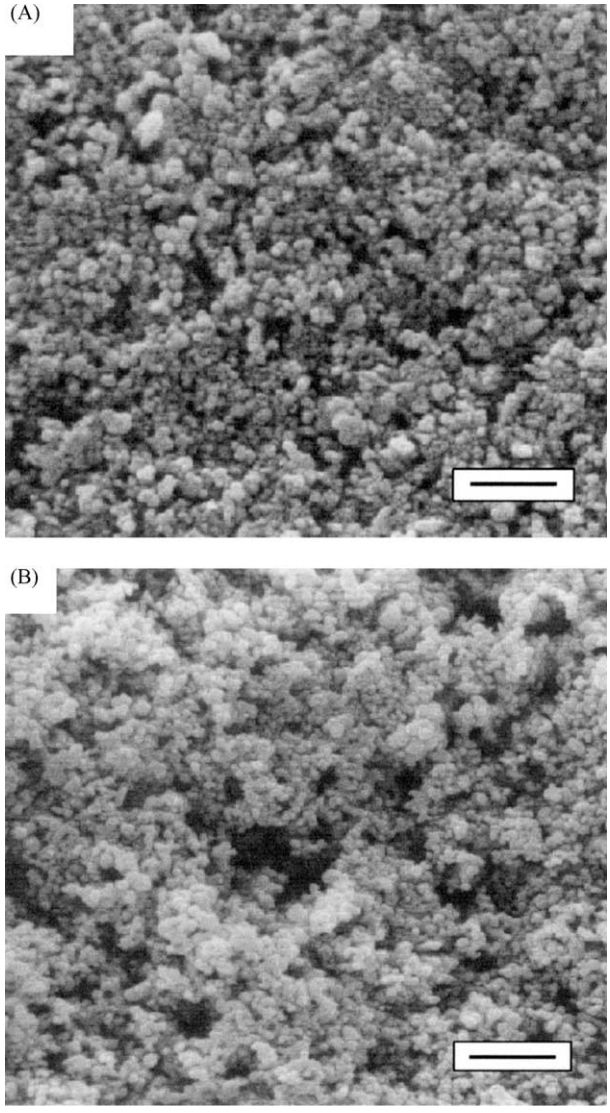

Fig. 1. SEM micrographs of the films (bar = 2 μm). Sample S1 (A), sample S2 (B).

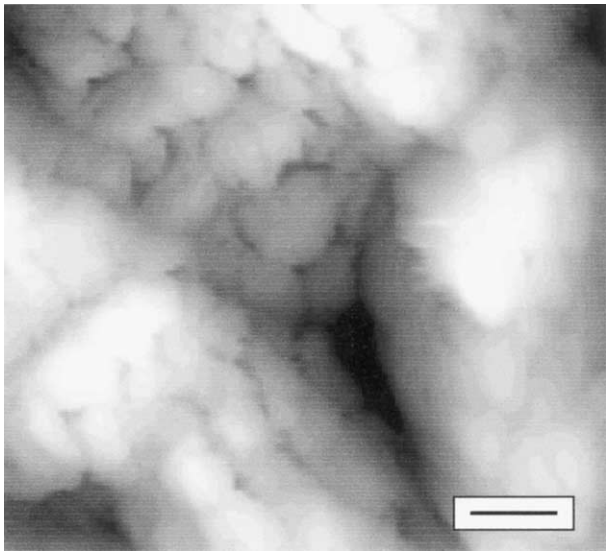

Fig. 2. STM image of sample S1 (bar = 100 nm).

changing the vacuum into oxygen flux ($t = 0$) and back into vacuum. In Fig. 3A—experiment carried out at 280 °C—after a quick increasing due to oxygen exposure, the electrical resistance is almost constant over a lapse of 700 s. On the other hand, for temperatures higher than 280 °C (Fig. 3B) a diminution in the resistance after a quick increasing is observed. In both cases the resistance decreases after the oxygen removal.

Fig. 4 shows electrical responses (resistance vs. time) of the sample with larger particle size after changing the vacuum into oxygen flux ($t = 0$) and back into vacuum. Fig. 4A and B show an electrical response similar to that observed in sample S1 at low temperature (Fig. 3A). When the temperature is increased at values close to 400 °C, a slow decreasing in the resistance with exposure time was registered (Fig. 4C). This behaviour is similar to that observed at lower temperatures in sample S1 (see Fig. 3B). However, in sample S2 a slower response to that of S1 is apparent.

Resistance versus time curves can be understood by considering that intergranular potential barriers are responsible for the observed electrical response. The rapid increase of the resistance, when samples are exposed to oxygen, indicates that equilibrium at the surface is quickly reached. The interaction of oxygen with grain surfaces produces the transfer of electrons from the bulk to the surface. From this process, the barrier height and the depletion width become larger and, as a consequence, the sample resistance increases. The subsequent slow change in the electrical response needs a more subtle discussion. In a previous work, we proposed that oxygen diffusion into the grains is responsible for these slow evolution in resistance by affecting the oxygen vacancies concentration and then the Schottky barrier widths.[11]

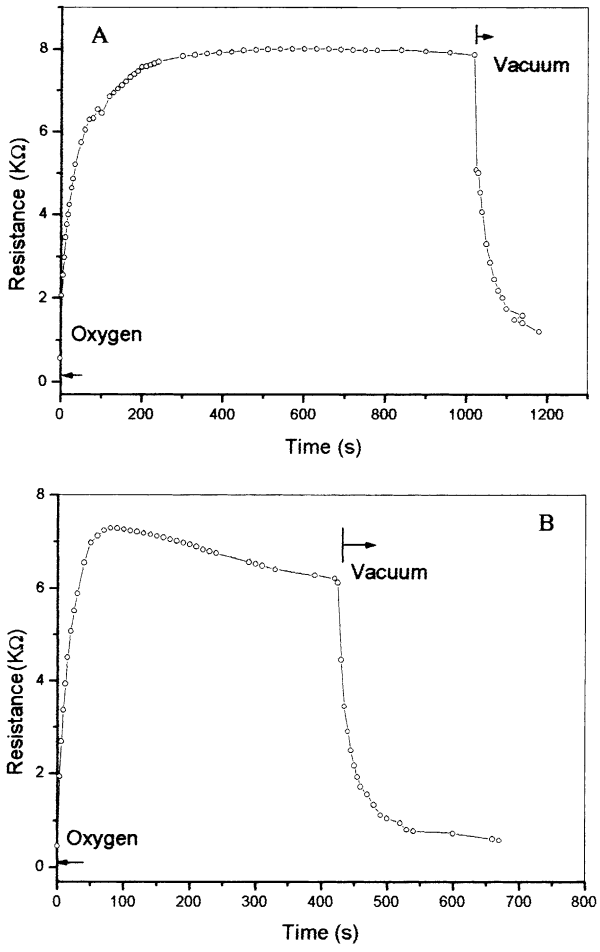

Fig. 3. Resistance vs. time curves of sample S1 for an oxygen pressure of 8.4 mmHg at 280 °C (A) and 320 °C (B).

It is generally accepted that oxygen vacancies in tin oxide act as electron donors and thus they tend to increase the conductivity of the film. A band model for large grains is shown in Fig. 5(a) in which Schottky barriers of height Φ at the grain surfaces determine the sample conductivity. After oxygen diffusion into the grain, Fig. 5(b), oxygen vacancy concentration is reduced, the depletion width of intergrain barriers becomes larger while the barriers heights are not altered. Thus, due to a lower electron density and wider barriers that reduce thermionic and tunnelling currents, the sample conductivity decreases. However, not always a reduction in the number of oxygen vacancies has this effect.[12] For small grains, see Fig. 5(c), depletion widths can be large enough to overlap. In this case, a diminution of the vacancy concentration reduces the intergrain barriers that electron must overcome to flow as seen in Fig. 5(d).

At temperatures higher than 270 °C—in the samples with small particle size—the oxygen diffusion into the grains is significant and the bottom of overlapped potential barriers increases. At lower temperatures the oxygen diffusion into the grains is very slow and the

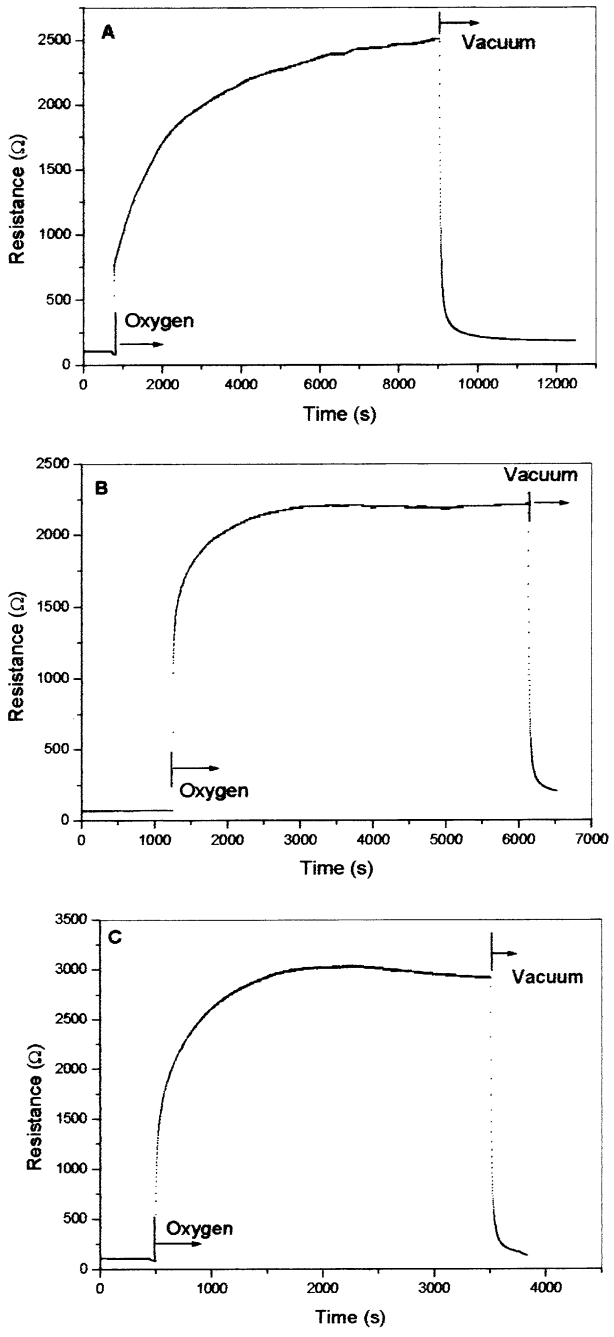

Fig. 4. Resistance vs. time curves of sample S2 for an oxygen pressure of 8.4 mmHg at 260 °C (A), 354 °C (B) and 405 °C (C).

oxygen vacancies annihilation is not enough to produce a relevant modification of the potential barriers in the time frame of the our experiments. Kamp et al. determined diffusivities of SnO_2 single crystals.[13] At odds with our results, they found that surface exchange reaction of oxygen on SnO_2 rather than diffusion of oxygen into their samples controls the conductivity. Our findings, however, indicate the presence of a second mechanism and experimental results are consistent with the interpretation of a slow diffusion of oxygen into the grains. We think that differences with the work of Kamp et al. can be attributed to the nature of the samples used.

On the other hand, after a first quick increasing, the sample with large particle size (S2) only presents a decrease in the resistivity when it is exposed to oxygen at temperatures close to 400 °C. In this sample, barriers are separated due to the large particle size, and then overlapping is only possible when oxygen diffusion into the grains is very important (temperatures as high as 400 °C). At low or moderate temperatures oxygen diffusion into the grains is not enough to produce the potential barrier overlapping, and then a monotonous increasing in the resistivity is observed.

The sample with larger particle size (S2) showed a relatively slower response than sample with smaller particle sizes (S1). This result could be explained by considering that sample S2 is thicker than S1. It has long been suggested that the response of a semiconductor gas sensor is related to reaction and diffusion of gas molecules inside gas sensing layers.[14] Since there is no reaction in the experiments presented here, only diffusion of the gas into the sensor layer has to be considered. In order to explain the temporary response of the sensors we will take into account that pores included in the films are fairly developed. Films have macropores (between grains and agglomerates) and mesopores (within agglomerates). Macropores have radius far larger than 100 nm and mesopores have radius ranging from 1 to 100 nm. It is known that diffusion through porous materials is typically described as either ordinary, Knudsen, or surface diffusion. Ordinary diffusion occurs when the pore diameter of the material is large in comparison to the mean free path of the molecules of the gas (in the macropores). Molecular transport through pores which are small in comparison to the mean free path of the gas is described as Knudsen diffusion (in the mesopores). In surface diffusion, molecules are adsorbed on the surface of the material and are subsequently transported from one site to another with a net flux in the direction of the decreasing concentration. This diffusion has been assumed to contribute little to the overall transport but it could be important in thin films consisting of very fine oxide grains.[4,15] Taking into account Knudsen diffusion (D_K) inside mesopores, and ordinary diffusion (D_o) inside macropores, the effective diffusion coefficient (D_e) depends on both diffusion processes.

Ordinary diffusion contributes to the total molecular transport through the macropores, it depends on the porosity of the particle and the length of the path along which the molecule travels. This diffusion coefficient can be expressed as

$$D_o = D.\theta/\tau, \quad (1)$$

where θ is the porosity and τ the tortuosity factor. Knudsen diffusion coefficient (D_K) is expressed as

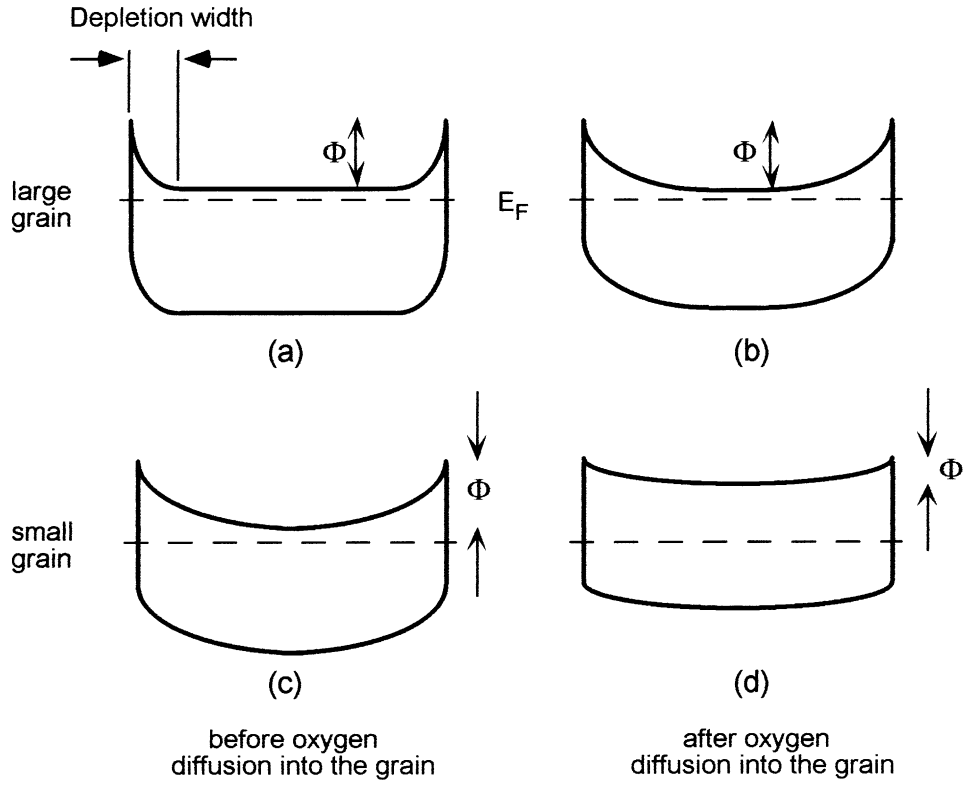

Fig. 5. Band diagrams showing the effect of decreasing the oxygen vacancy concentration in tin oxide grains. For large grains (a), when depletion layers do not overlap, a lower vacancy concentration implies a lower conductivity (b). For small grains (c), when depletion layers are overlapped, a lower vacancy concentration implies a larger conductivity (d).

$$D_K = 9700.r.\sqrt{T/M}, \tag{2}$$

where T is the temperature (K), r the pore radius pore (cm), and M the molecular weight of gas.

For the sake of simplicity, we will assume that the porous film can be represented by a straight channel structure. Thus, each channel is a round pore of radius r and length L. This effective diffusion is expressed by the following equation:

$$\partial C_A/\partial t = D_e\left(\partial^2 C_A/\partial x^2\right) \tag{3}$$

where x is the distance from the film surface, t is the time, C_A the gas concentration at x, t. The concentration profile of the gas can be obtained solving Eq. (3). Three boundary conditions are needed in order to determine the three integration constants involved. One boundary condition is $C_A = C_{A,s}$ at $x = L$, where $C_{A,s}$ is concentration of A in the surrounding atmosphere (assuming that the resistance to the mass transport in the gaseous phase is neglected), another condition is that there is not flux at the film–substrate interface, i.e. $\partial C_A/\partial x = 0$ at $x = 0$, the third boundary condition considers that the $C_{A,0} = 0$ at $t = 0$ in the film. Then, using the separation of variables method, Eq. (3) can be solved to give

$$\begin{aligned}\left(C_A - C_{A,0}\right)/\left(C_{A,s} - C_{A,0}\right) &= 1 - 4/\pi\sum_{n=0}^{\infty}(-1)^n/(2n+1)^2.\cos[(2n+1)\pi x/2L].\\ &\exp\left[-(2n+1)^2\pi^2 D_e t/\left(4L^2\right)\right]\end{aligned} \tag{4}$$

Then, the amount of oxygen transferred into the film at any time can be determined by integrating the concentration over the thickness. Therefore, the mass transferred at any time is

$$\begin{aligned}M_t = 2\left(C_{A,s} - C_{A,0}\right)L\Big\{1 - 8/\pi^2\sum_{n=0}^{\infty}1/(2n+1)^2.\\ \exp\left[-(2n+1)^2\pi^2 D_e t/\left(4L^2\right)\right]\Big\}.\end{aligned} \tag{5}$$

The maximum uptake of the film corresponds to the limit $t \to \infty$; i.e.

$$M_\infty = 2L\left(C_{A,s} - C_{A,0}\right). \tag{6}$$

The uptake relative to the maximum is given as

$$M_t/M_\infty = 1 - 8/\pi^2 \cdot \sum_{n=0}^{\infty} 1/(2n+1)^2 \cdot \exp\left[-(2n+1)^2\pi^2 D_e t/\left(4L^2\right)\right]. \quad (7)$$

According to this equation the time needed to reach the steady state is directly related to $D_e t/L^2$. Then, if we consider that $L = 100$ μm for sample S1 and $L = 440$ μm for sample S2, the S2 response is approximately twenty times slower than S1 assuming that D_e is the same for both types of samples. In fact this is the relation found in the experiments between the times needed to reach steady states.

It is known that D_o is about one order of magnitude larger than D_K, and that a higher porosity favours ordinary diffusion. Then, D_K is the controlling resistance of the process. Since this diffusion coefficient has a small variation between samples S1 and S2, D_e is practically the same. The Knudsen diffusion relevance was also assumed by Sakai et al. in their theory of gas-diffusion controlled sensitivity for thin films.[4] They considered that an inflammable gas moves inside the film by Knudsen diffusion, while it reacts with the adsorbed oxygen following a first-order reaction kinetic.

On the other hand, the sample S2 showed a higher R_{air}/R_{vacuum} relation than S1. This behaviour could be related to different conduction processes. As it was explained above, the sample S1 presents a small grain size and overlapped potential barriers, while the sample S2 presents a large grain size and separated potential barriers.

To gain confidence in the above interpretation, the evolution of conductance as a function of temperature was studied. In Fig. 6 conductance vs. 1/temperature curves for a sample with small particle size are presented. Conductance was measured by raising and then decreasing the temperature under oxygen reaching different final temperatures. For temperature ramps in a range below 160 °C, the conductivity in the cooling process is lower than in the heating process. This behaviour could be associated with the oxygen adsorption on the particle surface which produces a diminution in the sample conductivity. In this case, oxygen adsorption produces an increasing of the potential barrier height and then a reduction in the sample conductivity is observed. At these temperatures oxygen diffusion into the grains is not significant. Conversely, temperature ramps at temperatures higher than 220 °C produces a final effect of increasing the sample conductivity. At these temperatures the oxygen into the grains provokes an increasing in the bottom of the overlapped barriers and, as a consequence, the conductivity increases. These results are consistent with the curves presented in Fig. 3.

In Fig. 7 conductance vs. 1/temperature curves for a sample with larger particle size are presented. Experiments were performed as described above. In all the set of measurements conductance after cooling was lower than after heating. As it was previously discussed, in this sample the overlapping of the potential barriers is not expected. Also, oxygen diffusion into these thick samples is very slow and then in this dynamic experiment the overlapping of the potential barrier does not occur. As a consequence, only the effect of surface adsorption was detected.

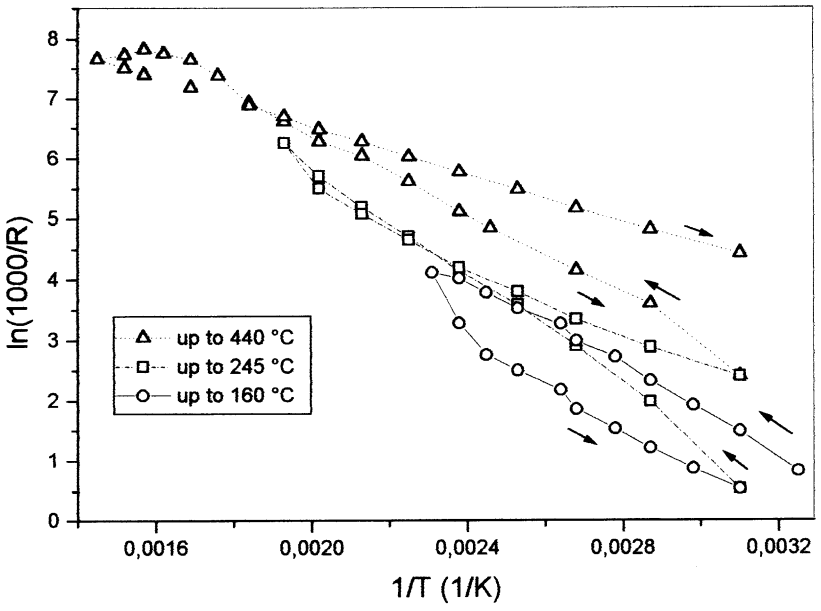

Fig. 6. Electrical conductance during heating and cooling under oxygen (8.4 mmHg) as a function of 1/temperature for sample S1.

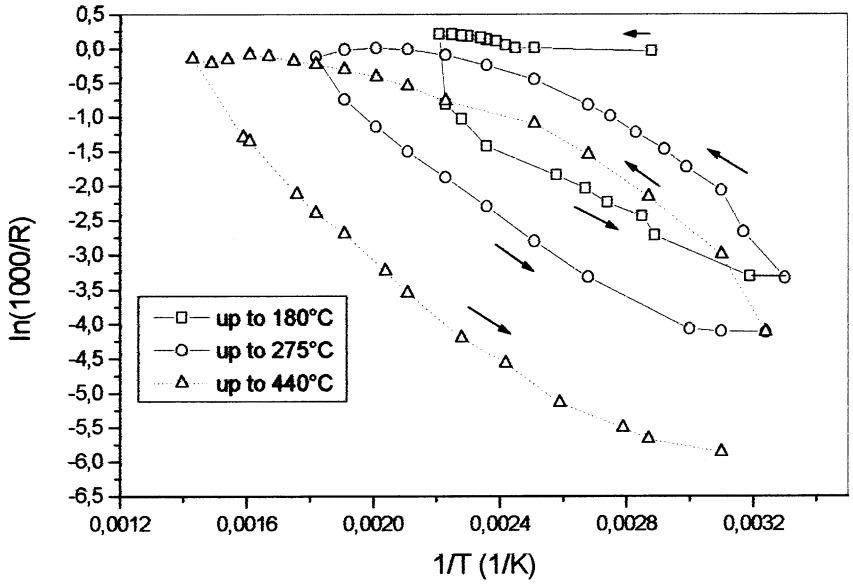

Fig. 7. Electrical conductance during heating and cooling under oxygen (8.4 mmHg) as a function of 1/temperature for sample S2.

4. Conclusions

From the experimental results, it is possible to conclude the following.

1. Thick films made from medium particle size of 0.4 μm have mostly overlapped potential barriers at the grain boundaries. When the film is exposed to an oxygen atmosphere, two processes take place. First, the oxygen adsorption provokes the increasing of the potential barrier height. After that, oxygen diffusion into the grains reduces the intergrain barriers height. Then, an increasing in the resistance and a subsequent decreasing in the resistance is observed.

2. Thick films made from medium particle size of 0.7 μm have mostly separated potential barriers at the grains. These samples present a monotonous increasing in the resistivity with the oxygen exposure times. Oxygen diffusion into the grains can produce the potential barrier overlapping only after large exposition times.

3. Transient behaviours through the films could be explained using a simple diffusion model. Effective diffusion was related to the Knudsen mechanism.

Acknowledgements

The authors want to thank Mr. Héctor Ascencio for his technical support and Dr. Patricia Suárez for the STM images acquisition.

References

1. Madou, M. J. and Morrison, R., *Chemical Sensing with Solid State Devices*. Academic Press, Inc, San Diego, 1989.
2. Cukrov, L. M., McCormick, P. G., Galatsis, K. and Wlodarski, W., Gas sensing properties of nanosized tin oxide synthesised by mechanochemical processing. *Sens. Actuators B*, 2001, **77**, 491–495.
3. Karthigeyan, A., Gupta, R. P., Scharnagl, K., Burgmair, M., Zimmer, M., Sharma, S. K. and Eisele, I., Low temperature NO_2 sensitivity of nano-particulate SnO_2 film work function sensors. *Sens. Actuators B*, 2001, **78**, 69–72.
4. Sakai, G., Matsunaga, N., Shimanoe, K. and Yamazoe, N., Theory of gas-diffusion controlled sensitivity for thin film semiconductor gas sensor. *Sens. Actuators B*, 2001, **80**, 125–131.
5. Maekawa, T., Suzuki, K., Takada, T., Kobayashi, T. and Egashira, M., Odor identification using a SnO_2-based sensor array. *Sens. Actuators B*, 2001, **80**, 51–58.
6. Lu, H., Ma, W., Gao, J. and Li, J., Diffusion-reaction theory for conductance response in metal oxide gas sensing thin films. *Sens. Actuators B*, 2000, **66**, 228–231.
7. Kanamori, M., Suzuki, K., Ohya, Y. and Takahashi, Y., Analysis of the change in the carrier concentration of SnO_2 thin film gas sensors. *Jpn. J. Appl. Phys.*, 1994, **33**, 6680–6683.
8. Shimizu, Y. and Egashira, M., Basic aspects and challenges of semiconductor gas sensors. *M.R.S. Bull.*, 1999, **24**, 18–24.
9. Gaggiotti, G., Galdikas, A., Kaciulis, S., Mattogno, G. and Setkus, A., Surface chemistry of tin oxide based gas sensors. *J. Appl. Phys.*, 1994, **76**, 4467–4471.
10. Moseley, P. T., Solid state gas sensors. *Meas. Sci. Technol.*, 1997, **8**, 223–237.
11. Blaustein, G., Castro, M. S. and Aldao, C. M., Influence of the frozen distributions of oxygen vacancies on tin oxide conductance. *Sens. Actuators B*, 1999, **55**, 33–37.
12. Vlachos, D. S., Papadopoulos, C. A. and Avaritsiotis, J. N., Dependence of sensitivity of SnO_x thin-film gas sensors on vacancy defects. *J. Appl. Phys.*, 1996, **80**, 6050–6054.
13. Kamp, B., Merkle, R. and Maier, J., Chemical diffusion of oxygen in tin oxide. *Sens. Actuators B*, 2001, **77**, 534–542.
14. Sakai, G., Baik, N. M., Miura, N. and Yamazoe, N., Gas sensing properties of tin oxide thin films fabricated from hydrothermally treated nanoparticles. Dependence of CO and H_2 response on film thickness. *Sens. Actuators B*, 2001, **77**, 116–121.
15. Hines, A. L. and Maddox, R. N., *Mass Transfer. Fundamentals and Applications*. Prentice Hall, NJ, 1985.